Analysis of the efficiency and potential collapse of the ensemble Kalman filter for marginal and joint posteriors

Matthias Morzfeld[1,2] and Daniel Hodyss[3]

[1]Department of Mathematics, University of California, Berkeley;
[2]Lawrence Berkeley National Laboratory;
[3]Naval Research Laboratory, Monterey.

Abstract

In data assimilation one updates the state of a numerical model with information from sparse and noisy observations of the model's state. A popular approach to data assimilation in geophysical applications is the ensemble Kalman filter (EnKF). An alternative approach is particle filtering and, recently, much theoretical work has been done to understand the abilities and limitations of particle filters. Here we extend this work to EnKF. First we explain that EnKF and particle filters solve different problems: the EnKF approximates a specific marginal of the joint posterior of particle filters. We then perform a linear analysis of the EnKF as a sequential sampling algorithm for the joint posterior (i.e. as a particle filter), and show that the EnKF collapses on this problem in the exact same way and under similar conditions as particle filters. However, it is critical to realize that the collapse of the EnKF on the joint posterior does not imply its collapse on the marginal posterior. This raises the question, which probability, the joint or marginal, is of greater importance in geophysical applications. We argue that the marginal is the more practical object in many geophysical applications and in particular in numerical weather prediction, which explains the usefulness of EnKF in these applications.

1 Introduction

Many applications in geophysics, in particular numerical weather prediction, require that one updates the state of a numerical model with information from sparse and noisy observations of the state (see, e.g. [9, 17, 18, 26, 40]). The theory for these data assimilation problems uses conditional probability and Bayes' rule to define posterior probability densities that combine the information from the model with the observations.

With this paper, we want to bring to attention that there are two posterior probability densities of general interest, and that a careful distinction between these two densities is important for the analysis of the efficiencies of numerical data assimilation techniques. There is a joint posterior that describes the model's state history through time, conditioned on all the observations up to the present time. A marginal of this posterior describes the probability of the state at the current time, conditioned on all observations up to this time. Throughout this paper, we will refer to these densities as the *joint posterior* and the *marginal posterior*, respectively.

We analyze, discuss and compare the efficiencies of numerical data assimilation methods on the marginal and joint posterior densities. We point out that particle filters [3, 15] and (ensemble) Kalman filters (EnKF) [17, 24, 25] solve two different problems: particle filters sample the joint posterior, while EnKF samples the marginal posterior (approximately). In our analysis and discussion, we focus on the difficulties that a large state dimension causes in these two classes of numerical data assimilation methods. Variational data assimilation, which finds the state of maximum posterior probability (of either the joint or marginal posterior, see, e.g. [6, 38]), will not be discussed. The goal of this work is rather to improve the understanding for the requirements of successful application of the EnKF by extending the methods to diagnose the quality and behavior of particle filters

to EnKF. Thus, our main goal is to develop new theory and diagnostics to lead the development of the EnKF into nonlinear and high-dimensional problems.

We extend the theoretical results for the limitations of particle filters to EnKF. This is where the careful distinction between joint and marginal posteriors becomes important. Particle filters sample the *joint posterior* sequentially, see e.g. [1, 3, 12–14, 16, 20, 31, 33, 41–44]. Attached to each sample, or particle, is a weight, and the variance of the weights determines the efficiency of the particle filter. If the variance is large, then the filter collapses onto one particle and, therefore, fails. By extending the methods of particle filters, developed in [5, 7, 11, 36, 37], to the weighted EnKF, first proposed in [34], we find the conditions for the collapse of the EnKF as a sequential sampling algorithm for the *joint posterior*. We show with an example that EnKF collapses in the same way as particle filters, but under broader conditions. This is perhaps not surprising since even the optimal particle filter [16, 31, 44] collapses [11, 36]. The optimal filter however collapses due to errors one made in previous assimilation cycles. This implies that the collapse of particle filters on the joint posterior is unavoidable unless one is willing to update past states in view of current observations. We show that the EnKF is no exception to that rule.

We explain that the collapse of EnKF on the *joint posterior* does not imply its collapse on the *marginal posterior*. The collapse of EnKF (and other particle filters) on the *joint posterior* is due to errors one made in previous assimilation cycles. The marginal posterior however describes the state at the observation time and, therefore, is insensitive to errors one made in previous assimilation cycles. When applied to the marginal posterior, the EnKF (and possibly particle filters) can avoid a collapse due to errors in the past. We derive the weights of EnKF with respect to the marginal and show that the EnKF, with optimal localization and inflation, is an optimal sampling algorithm for the marginal posterior, if the problem is linear and Gaussian. In nonlinear/non-Gaussian problems, the weights are difficult to compute unless the observations are collected in sync with the model's time stepper (which is often not the case because the time-step of the model is typically smaller than the time-window between observations). We illustrate the weights with several numerical examples, including the Lorenz '63 equations [32]. The weights represent a new diagnostic tool for EnKF and may be useful for tuning localization, inflation, or the ensemble size.

The optimality of EnKF on the marginal posterior of linear/Gaussian problems suggests that EnKF can be efficient for mildly nonlinear problems as well. In fact, the EnKF is known to perform well with small ensembles in several high-dimensional problems. However, it was reported in [19], that the ensemble size scales quadratically with the state dimension, or else the sampling error becomes unbounded. Since the state dimension in geophysical applications often exceeds 10^6, EnKF would be impractical in these problems if this scaling was practical (since using e.g. 10^{12} ensemble members, each of dimension 10^6, is not feasible). Here we offer a possible explanation for the good performance of EnKF in high-dimensional problems by exploring connections of EnKF with the theory in [11], where a feasibility condition for data assimilation is discussed.

Our results underline the importance of the question which probability, the joint or marginal posterior, is of greater significance in geophysical data assimilation. In numerical weather prediction, one can argue that the main goal is to compute an accurate forecast. With this goal in mind, a good knowledge of the current state is required, however mistakes one made in previous forecasts or assimilation cycles are irrelevant. Thus, the marginal posterior is more practical than the joint posterior, and EnKF may be more appropriate than particle filters. However, other applications may require the joint posterior (at least over a time-window), and, in theses cases, our analysis shows that EnKF is a suboptimal choice because a well-designed particle filter can be more broadly applicable to this problem than EnKF.

2 Review of particle filters, EnKF, and feasible data assimilation

We consider data assimilation problems of the form

$$x^n = f(x^{n-1}) + d^n, \tag{1}$$
$$z^n = Hx^n + e^n, \tag{2}$$

where $n = 1, 2, 3, \dots$ represents a discrete time, x is a real m-dimensional vector, f is a smooth m-dimensional vector function, z is a real k-dimensional vector, and where H is a $k \times m$ matrix; the random variables d^n and e^n are independent identically distributed (iid), i.e. e^n is independent of d^n for every n and d^i, or e^i, and d^j, or e^j, are independent for $i \neq j$. We assume that e^n and d^n are Gaussians with mean zero and constant (in time) covariance matrices Q and R:

$$d^n \sim \mathcal{N}(0, Q), \quad e^n \sim \mathcal{N}(0, R).$$

The covariances Q and R are $m \times m$ respectively $k \times k$ symmetric positive definite (SPD) matrices. Thus, our analysis excludes data assimilation problems with a perfect (deterministic) model for which $Q = 0$. We caution the reader not to attempt to examine the $Q \to 0$ limit in our results. While this is tempting we will discuss below why this cannot be done. The analysis with deterministic models will be given elsewhere in the future.

The goal in data assimilation is to update the state x of the model (1) in view of the noisy observations z in (2). There are two approaches to this problem. On can consider the conditional random variable $x^{0:n}|z^{1:n}$, which describes the *state trajectory* up to time n, given the observations up to time n (as is customary we assume that no observations are available at time $n = 0$ and write $y^{1:n}$ for a set of vectors $\{y^1, \dots, y^n\}$). This random variable is specified by the **joint posterior**

$$p(x^{0:n}|z^{1:n}). \tag{3}$$

On can also focus on the *state at observation time* rather than the entire trajectory and consider the **marginal posterior**

$$p(x^n|z^{1:n}) = \int \dots \int p(x^{0:n}|z^{1:n})\, dx^0 \dots dx^{n-1}. \tag{4}$$

Note that the joint posterior describes the history of the state up to time n, $x^{0:n}|z^{1:n}$, which is a random variable of dimension $m \cdot n$. If large data sets are considered (large n), then the dimension of the joint posterior can be large even when the state dimension, m, is small. In geophysical data assimilation, one often encounters large data sets (e.g. long records of past weather data), however forecasts must be provided frequently. The marginal posterior, $x^n|z^{1:n}$, on the other hand is of dimension m, independently of n. While m may be large, solving for the marginal posterior is a lower-dimensional problem than solving for the joint posterior.

2.1 Ensemble Kalman filters

The Kalman filter [24, 25] recursively computes the mean and covariance of the *marginal posterior* (4). The computations require dense linear algebra on matrices of the size of the state dimension, which is impractical in large-dimensional problems. In these cases, the EnKF can be used. The EnKF makes use of a Monte Carlo (MC) approximation of a forecast probability to reduce the computational requirements of Kalman filtering [17, 39].

Specifically, let x_j^{n-1}, $j = 1, \dots, M$ be samples of the marginal posterior $p(x^{n-1}|z^{1:n-1})$ at time $n-1$. The collection of samples is usually called the ensemble, and each sample is an ensemble

member. The ensemble is evolved to time n using the model (1) on each member, and one obtains the forecast ensemble

$$\hat{x}_j^n = f(x_j^{n-1}) + d_j^n,$$

where d_j^n is a sample of d^n. Let

$$X_n = \frac{1}{M-1}\sum_{j=1}^{M}(x_j^n - \bar{x}^n)(x_j^n - \bar{x}^n)^T, \tag{5}$$

be the sample covariance of the forecast ensemble. With this covariance (perhaps localized and inflated), define the Kalman gain

$$K_n = X_n H^T (H X_n H^T + R)^{-1}, \tag{6}$$

which is used to compute the "analysis ensemble":

$$x_j^n = \hat{x}_j^n + K_n\left(\hat{z}_j^n - H\hat{x}_j^n\right), \tag{7}$$

where $\hat{z}_j^n$ is a "perturbed observation" obtained from

$$\hat{z}_j^n = z^n + e_j^n,$$

where e_j^n is a sample of e^n. The sample mean and sample covariance of the analysis ensemble approximate the mean and covariance of the marginal posterior $p(x^n|z^{1:n})$.

In linear/Gaussian problems, the marginal posterior is Gaussian and EnFK samples this Gaussian (asymptotically, for large ensemble sizes). Nonlinear dynamics however are likely to make the posterior probability non-Gaussian. In fact, it was shown in [21] that the EnKF state estimate can be understood as the first-order approximation of a Taylor-series of the posterior mean. This requires that (i) the posterior is symmetric but not necessarily Gaussian; and (ii) that the difference between the observation and the prior mean is not too large. These two assumptions lead to the typical requirements for the successful application of the EnKF: it is agreed upon that the EnKF "does not work" if the nonlinearity is too strong or the time between observations is too large. These two issues are in fact connected. A numerical model may behave almost linearly over short time-scales, but exhibit strongly nonlinear behavior over longer time-scales. Thus, the effects of nonlinearity are often amplified if the time between observations is not small (compared to the time-scale that governs the nonlinear behavior), and a strong nonlinearity will typically develop asymmetries in the posterior which will render its state estimate inaccurate.

Below we investigate the efficiency of EnKF on the marginal and joint posterior. We focus on the perturbed observations implementation of EnKF, as outlined above, however other implementations of EnKF are also available [2, 8, 39].

2.2 Particle filters

The goal of this paper is to connect the theory of the limitations of particle filters with EnKF, to identify situations in which EnKF can be expected to be efficient, reliable and accurate. The basics of particle filters are reviewed below.

In particle filtering one uses sequential importance sampling [10, 27] to construct an empirical estimate of the *joint posterior* (3). This joint posterior satisfies the recursion

$$p(x^{0:n}|z^{1:n}) = p(x^{0:n-1}|z^{1:n-1})\,\frac{p(x^n|x^{n-1})p(z^n|x^n)}{p(z^n|z^{1:n-1})}. \tag{8}$$

The empirical estimate consists of a collection of weighted samples, such that expected values of functions of $x^{0:n}|z^{1:n}$ can be approximated by weighted averaging over the samples. The samples are generated using an importance function of the form

$$\pi(x^{0:n}; z^{1:n}) \propto \pi^0(x^0) \prod_{k=1}^{n} \pi^k(x^k|z^{1:k}, x^{0:k-1}). \tag{9}$$

The key useful feature of an importance function of the form (9) is that it is a sequence of products of functions, similar to the sequence of products one finds in the joint posterior. With an importance function of this form, one can thus derive a sequential data assimilation algorithm in which only the most recent function needs to be updated when a new observation is collected. At each step k, the update $\pi^k(x^k; z^{1:k}, x^{0:k-1})$ is used to propose samples x_j^k, which are appended to the samples of $x_j^{0:k-1}$ to extend the trajectory to time k. With an importance function of the form (9), the weights satisfy the recursion

$$w^n \propto \frac{q(x^{0:n}|z^{1:n})}{\pi(x^{0:n}|z^{1:n})} \propto w^{n-1} \frac{p(x^n|x^{n-1})p(z^n|x^n)}{\pi^n(x^n|z^{1:n}, x^{0:n-1})}, \tag{10}$$

and account for the fact that one draws samples from the importance function $\pi(x^{0:n}|z^{1:n})$, rather than from the joint posterior $p(x^{0:n}|z^{1:n})$. After each step, the weights are normalized such that their sum is one. This normalization makes it possible to sample probabilities which are known only up to a multiplicative constant (which is usually the case).

Various choices for the updates $\pi^k(x^k|z^{1:k}, x^{0:k-1})$ lead to the various particle filters in the literature, each with different weights (see, e.g. [3, 12–14, 16, 20, 31, 33, 42–44]). The behavior of the weights determines the efficiency of a particle filter. Specifically, it is shown in [5, 7, 36, 37] that the variance of the negative logarithm of the unnormalized weights must be small or else the particle filter "collapses" onto one sample. To understand this condition better, suppose that the variance of the weights at step n before normalization is large. The large variance implies that $\min_j w_j^n \ll \max_j w_j^n$. After normalization, one thus obtains one sample with a weight (close to) one while the $n-1$ remaining samples all have weights (close to) zero. This means that one has obtained only a single effective sample. In contrast, suppose that the variance of the weights before normalization is small. This implies that the weights must be nearly equal and therefore each member of the ensemble can be considered as a nearly equally likely draw from the posterior, which is the desired situation.

The collapse of particle filter has been studied carefully recently [5, 7, 36, 37]. In particular, for large dimensional systems, it was shown that the variance of the negative logarithm of the unnormalized weights at each step must remain finite as the dimension m of the problem goes to infinity, or else a particle filter collapses at that step. In summary,

$$var(\gamma^n) < \infty, \quad \text{as } m \to \infty,$$

where

$$\gamma_\pi^n = -\log\left(\frac{p(x^n|x^{n-1})p(z^n|x^n)}{\pi^n(x^n|z^{1:n}, x^{0:n-1})}\right),$$

is a condition for a successful particle filter.

We wish to point out that the "equivalent weights particle filter" (EWPF) [1,41] is not a particle filter with an importance function of the form (9) and, therefore, EWPF may not converge to the posterior as the number of particles goes to infinity. EWPF achieves a small variance of the weights at the cost of biases in the estimates of the posterior (e.g. a particle filter that suggests $x_j = 0$ for $j = 1, \ldots, M$ has "eqivalent weights", however an approximation of the posterior with this set of equivalent particles is not useful). Our analysis does directly apply to EWPF.

2.3 Review of feasible data assimilation

While the theoretical solution of data assimilation problems is clear, the practical use of data assimilation requires answers to questions that are independent of how the data assimilation is implemented numerically. For example: (*i*) What conclusions can one draw from the posterior, especially if the noises in the model or data are large? (*ii*) How do the errors one can expect in posterior state estimates scale with the dimension of the problem? These questions, concerning the *data assimilation problem* rather than its numerical solution, were raised in [11]. Below we connect this theory to the efficiency of EnKF on the marginal posterior. We review the main findings of [11] so that this paper can be read independently.

The basic idea can be explained with a one-dimensional problem. Suppose the posterior has a variance that is large, e.g. the standard deviation is on the order of the state itself. In this case, the result of a data assimilation (even with a perfect algorithm) is that, in view of the model and the data, all one can say about the state is that there is noise (e.g. it may rain or the sun may shine, while at the same time it may be hot or cold). This result is not useful, in particular if a posterior based forecast is needed. An intuitive condition for feasibility of data assimilation in one dimension is, therefore, that the posterior standard deviation is small compared to the state of the system (i.e. the noise is small compared to the mean). Matrix norms can be used to extend this idea to high-dimensional systems: a data assimilation problem is feasible, if the posterior covariance matrix is "not too large" in a suitable matrix norm. In principle, this definition is applicable to data assimilation with the joint posterior (as in particle filters) or with the marginal posterior (as in EnKF).

We now focus on feasibility with respect to the *marginal posterior*, since the marginal is the more practical object in numerical weather prediction (where accurate forecasts are needed, rather than accurate reconstructions of the weather record over several days, months or years). We require that the problem is linear and Gaussian, because it allows us to make rigorous statements. A linear Gaussian problem is of the form (1)-(2), but with a linear model

$$x^n = Ax^{n-1} + d^n, \tag{11}$$

where A is an $m \times m$ matrix. The marginal posterior of such a data assimilation problem is Gaussian and its uncertainty is described by the marginal posterior covariance, which can be obtained by the Kalman filter [24, 25]. Given the marginal posterior covariance P_{n-1} at time of $n-1$, the KF updates this covariance to time n by

$$X_n = AP_{n-1}A^T + Q, \tag{12}$$

$$P_n = (I_m - K_nH)X_n, \tag{13}$$

where I_m is the identity matrix of order m and where K_n is the Kalman gain in (6). Under mild assumptions of d-detectability and d-stabilizability [30], the marginal posterior covariance P_n approaches a steady state, so that, for $n \to \infty$,

$$P_n \to P = (I_m - KH)X,$$

where X is the unique SPD solution of the discrete algebraic Riccati equation

$$X = AXA^T - AXH^T(HXH^T + R)^{-1}HXA^T + Q, \tag{14}$$

and where

$$K = XH^T(HXH^T + R)^{-1},$$

is the steady state Kalman gain. Note that we do not use the Kalman filter as a numerical method for data assimilation, but rather as a tool to derive large n asymptotics for the marginal posterior covariance. Lastly, we understand that this steady-state covariance matrix is not so clearly defined in nonlinear problems. Nevertheless, even in nonlinear problems, a data assimilation algorithm obtains a balance between error growth and variance reduction from observations, which is essentially what equation (14) describes.

In steady state, i.e. for large enough n, a (linear) data assimilation problem is thus feasible if the steady state covariance matrix is small in a suitable matrix norm. In principle, any matrix norm can be used (since all norms on finte-dimensional vector spaces are equivalent), however it is explained in [11] that the Frobenius norm, defined as

$$||P||_F = \sqrt{\sum_{i=1}^{m} \lambda_i^2}, \tag{15}$$

where λ_i, $i = 1, \ldots, m$, are the eigenvalues of the $m \times m$ (covariance) matrix P, is a natural choice. The reason is that Khinchin's theorem connects the Frobenius norm with correlations (see, e.g. [10]). The theorem states that correlations imply a small Frobenius norms of covariance matrices. Specifically, a correlated covariance matrix has a red eigen-spectrum and, therefore, its Frobenius is dominated by the largest eigenvalues. By contrast, an uncorrelated covariance matrix has a white spectrum and, therefore, its Frobenius norm is not dominated by any subset of eigenvalues. Thus, if the Frobenius norm of the posterior covariance matrix is small, then one can project the matrix onto a lower-dimensional space spanned by the eigenvectors connected with the large eigenvalues. This motivates to define an "effective dimension" [5,7,36,37] of a linear Gaussian data assimilation problems by

$$m_{\text{eff}} = ||P||_F.$$

While the term "dimension" may be somewhat confusing, we keep this terminology here to be in line with previous publications on this topic. Specifically, the effective dimension is not a dimension in the usual sense, but rather describes the effects of noise. For example, the effective dimension of a scalar Gaussian with standard deviation σ is $m_{\text{eff}} = \sigma$. In an m-dimensional state-space, the posterior covariance may have $k < m$ non-zero eigenvalues, so that the effective dimension is $m_{\text{eff}} = \sqrt{\sum_{i=1}^{k} \lambda_j^2}$ which is not necessarily equal to k, which is the dimension of the (stochastic) space we are dealing with. The effective dimension takes into account the stochasticity in each actual dimension and, therefore, can be less or larger than the dimension of the state-space.

By using the Frobenius norm to describe feasible data assimilation, we reflect the (empirically) well-known fact that correlations between state variables lead to fewer effective degrees of freedom and, therefore, to an "easier" data assimilation problem.

In practice, one needs to determine how large a Frobenius norm can be tolerated for feasible data assimilation. The precise threshold value depends on the problem and accuracy requirements, as well as on the typical scales in the problem and the computing resources. However, if one is interested in feasibility of data assimilation in high-dimensions, then it is natural to consider the asymptotic behavior for large dimensions (large m), and to define a feasible problem as one in which the posterior covariance remains finite (in Frobenius norm) as the dimension of the problem becomes infinite:

$$m_{\text{eff}} \doteq ||P||_F < \infty, \quad \text{as } m \to \infty.$$

This limit, $m \to \infty$, is of particular interest in numerical weather prediction and other applications in which the data assimilation problem involves a partial differential equation (PDE), and has been

used in connection with the limitations of particle filters before [5, 7, 36, 37] (see also the review of particle filters above). The reason is that the state is defined on a mesh, and the dimension m of the problem depends on this mesh, because the mesh is refined as m increases. The errors naturally start to correlate when the mesh is refined so that, By Khinchin's theorem, correlations imply a small Frobenius norm of the matrices Q and R. It was shown in [11] that small Frobenius norms of Q or R imply a small effective dimension. Thus, the physical interpretation of a feasible problem is one in which the errors correlate on a fine mesh. The issue of course is that in geophysics the grid resolution beyond which the Frobenius norm has converged may be so small as to be computationally intractable. We do not explore these issues of under-resolved dynamics and its impact on data assimilation here and assume throughout that the model problems we wish to solve are fully resolved (see [23] for further discussion).

Finally, note that the conditions for feasibility defined here may be harder to satisfy than, for example, the more typical condition that the posterior covariance be smaller than the climatological covariance. The reason is as follows. Suppose the climatological covariance matrix is large (in Frobenius norm), and that one could reduce it via data assimilation to find a posterior covariance that is smaller than the climatological covariance. While it may be true that the Frobenius norm of the climatological covariance is smaller than that of the posterior covariance, it may still be so large that reasonable inferences about future states are impossible. On one hand, one might assert that data assimilation is successful in the sense that the covariance was reduced, on the other hand, one might assert that data assimilation is infeasible in the sense that one may not be able to use the posterior to make an accurate forecast. We illustrate the above theory with two examples.

2.3.1 Uncorrelated linear Gaussian example

We consider a linear Gaussian problem of the form (2) and (11) with

$$A = I_m,\ H = I_m,\ Q = qI_m,\ R = rI_m, \tag{16}$$

where q and r are positive scalars; the dimension $m = k$ of the problem can be varied. This system has attracted much attention in the literature, in particular with respect to the limitations and efficiencies of particle filters, see, e.g. [5, 7, 11, 36, 37]. The systems' marginal posterior covariance matrix is diagonal

$$P_n = p^n I_m,$$

where $p^n > 0$ is a scalar that depends on q and r, as well as in the covariance of x^{n-1}. For large enough n, the system reaches a steady state so that $P_n \to P$. The steady state marginal posterior covariance can be computed by solving the Riccati equation (14):

$$P = \frac{\sqrt{q^2 + 4qr} - q}{2} I_m. \tag{17}$$

Its Frobenius norm is $||P||_F = p\sqrt{m}$. The effective dimension remains bounded as $m \to \infty$ if

$$\frac{\sqrt{q^2 + 4qr} - q}{2} \sqrt{m} = \text{Const.}. \tag{18}$$

Feasibility of data assimilation thus implies a balance condition between the noises in the model and data, represented by q and r. Setting the constant in (18) equal to one (because this is sufficient to show the qualitative behavior) allows us to simplify the condition for feasible data assimilation

$$r \leq \frac{\sqrt{m}q + 1}{mq}. \tag{19}$$

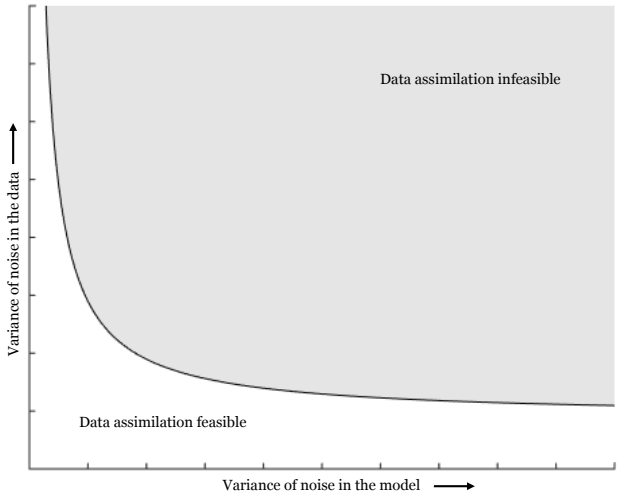

Figure 1: Condition for feasible data assimilation with the marginal posterior.

More generally, the constant should be a variance below which we believe that data assimilation is feasible (which is problem dependent). The feasibility condition is illustrated in figure 2, where we show the region in q-r-space for which (19) holds in white, and the region in which the condition does not hold in grey. In short, feasibility in data assimilation requires that not both sources of noise, in the model and observations, be large simultaneously, or else information about the state is drowned by excessive noise (see [11] for more detail). This result is confirmed in practice, which underlines the validity of the large m analysis.

On the other hand, the result that data assimilation with (16) is infeasible may be counter-intuitive, because the example is a collection of m independent scalar problems, each of which should be feasible. There are two reasons why the theory labels this collection of scalar problems as infeasible. The first is that the Frobenius norm is invariant under rotation. Thus, the analysis can not distinguish between the uncorrelated system (16), and a rotated version of it, such that in rotated coordinates the system is no longer diagonal. However, when the system is uncoupled into m scalar sub-problems, one makes use of the diagonal structure in the problem and a particular set of coordinates that exposes this structure. The analysis however cannot capture the diagonal structure, and, thus, labels the problem as infeasible, since other uncorrelated problems without the diagonal structure are in fact infeasible.

The second reason is that our definition of feasibility is strict and predicts a large overall error, even though each subsystem has a small error. The reason is that small errors add up to large errors. In particular, as m becomes large, it becomes increasingly likely that the error in one of the (scalar) subsystems is large. The above definition of feasibility finds that unacceptable, and labels the situation as infeasible. The situation is in fact analogous to the various kinds of convergence e.g. of infinite series: a series may converge in the L^2-norm, but may fail to converge in the L^∞-norm. Defining the uncorrelated example as feasible because the error in each component can be expected to be small (on average over the subsystems) is similar to using convergence in L^2-norm, while the definition of feasibility based on the Frobenius norm is more strict. Moreover, one can think of the requirement that the variance of the noise in each subsystem must decay with the system dimension (see equation (18)) as mimicking the effects of correlation in an uncorrelated system.

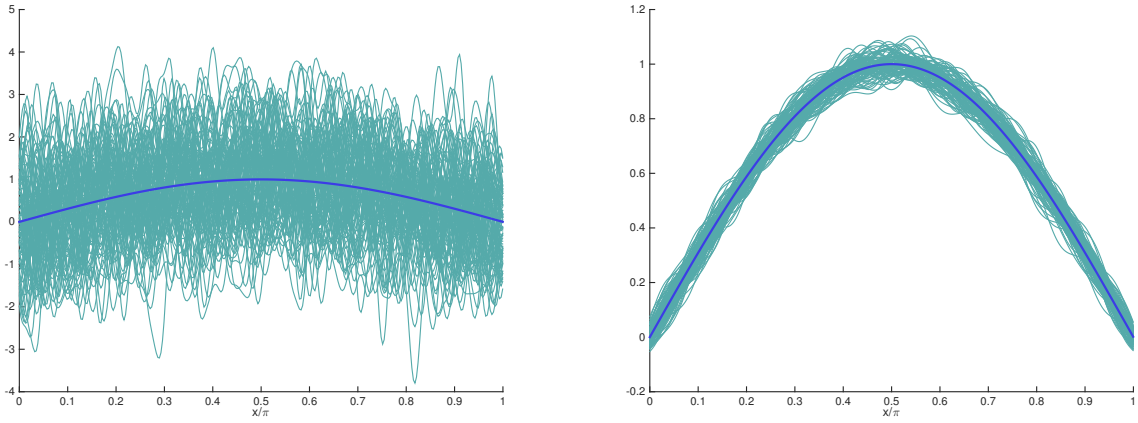

Figure 2: Left: a posterior covariance with a large Frobenius norm. Right: a posterior covariance with a small Frobenius norm. Turquoise: 100 posterior samples (one of which is the "true" state). Blue: posterior mean. Note the different scales of the y-axis.

2.3.2 Correlated Gaussian example

We now consider an example with correlations in the posterior. Suppose that the result of a data assimilation is a Gaussian posterior with mean $\sin(x)$ on $x \in [0, \pi]$. We consider two scenarios defined by two covariance structures: an exponential and a squared exponential covariance function respectively:

$$C_1(x_1, x_2) = \sigma_1 \exp\left(-\frac{(x_1 - x_2)^2}{2L_1^2}\right), \quad C_2(x_1, x_2) = \sigma_2 \exp\left(-\frac{|x_1 - x_2)|}{2L_2}\right).$$

Here $\sigma_1 = 0.01$, $L_1 = 0.01 \cdot \sqrt{50}$, $\sigma_2 = 0.5$ and $L_2 = 0.01 \cdot 2$. Note that both posteriors show correlations however the correlations in C_1 are stronger. We discretize the posterior on a uniform grid with $\Delta x = 0.01$, so that the state-dimension is $m = 315$. The Frobenius norm of the discretization of C_1 is $||P_1||_F = 0.62$, and for the discretization of C_2 we find a much larger Frobenius norm $||P_2||_F = 17.88$. The theory thus suggests that the problem with posterior covariance P_1 is more feasible, or easier to solve, than the problem with posterior covariance P_2.

This is illustrated in figure 1, where we plot 100 samples of the posteriors (in turquoise) as well as the mean (in blue). The samples of the posterior can be interpreted as the current weather. The blue line is, on average over many instances of the current weather, the best approximation of the current weather. However, the mean has little in common with the actual weather if the Frobenius norm is large (left). The mean is a good approximation of the current weather if the Frobenius norm is small (in the sense that the approximation is large/small where the current weather is large/small).

The reason is that the samples from the Gaussian with P_2 (large Frobenius norm) exhibit a large variation from the mean (and from each other) and, therefore, spread out in space to cover a large area. Thus, the various weather situations of the posterior (i.e. after the analysis) are different from one another and, therefore, will also lead to different forecasts. The posterior is more informative when the Frobenius norm is small. In this case, the samples are close together and do not deviate as much from the mean (and each other). Moreover, the various samples all exhibit common features. For example, all samples are large in the center of the domain and small at the boundaries. The state estimate (e.g. based on the mean) is more accurate if the Frobenius norm is

small, and one can also expect that the forecasts are more accurate in this situation. In this sense, data assimilation is feasible if the Frobenius norm is small and infeasible if the Frobenius norm is large.

It should however be pointed out that both problems are feasible for large m (by the definition above), since both the exponential and squared exponential covariance functions lead to covariance matrices with a decay of the eigenvalues so that the effective dimension remains bounded even as the dimension goes to infinity ($\Delta x \to 0$). The example underlines that the large m asymptotics may not be enough to determine feasibility of data assimilation in practice where information about typical scales of the state vector and relative errors are needed.

3 The collapse of EnKF on the joint posterior

As explained in the review above, the EnKF samples the *marginal* posterior (approximately). However, one can attach weights to the EnKF ensemble such that the weighted ensemble is distributed according to the *joint* posterior. Thus, one can view the EnKF as a particle filter for which the importance function is defined by the EnKF step. In this context, one can study the collapse of EnKF on the *joint posterior*.

The weighted EnKF for the joint posterior has already been described in [34]. The idea is to find the importance function from which the EnKF draws its ensemble. The ratio of the joint posterior and the EnKF importance function gives the weights attached to the EnKF ensemble members. The importance function for the EnKF is of the form (9) with $\pi^n(x^n|x_j^{n-1}, z^n)$ being a Gaussian that can be read off of equation (7) (see also [34]):

$$\pi^n_{j,\ \mathrm{EnKF}}(x^n|x_j^{n-1}, z^n) = \mathcal{N}\left(\mu_j^n, \Sigma_j^n\right), \tag{20}$$

where

$$\mu_j^n = (I - K_n H) f(x_j^{n-1}) + K_n z^n, \quad \Sigma_j^n = (I - K_n H) Q (I - K_n H)^T + K_n R K_n^T.$$

A related construction using Kernel density estimation at each step is discussed in [28]. Note that the importance function takes the state at the previous time $n-1$ and maps this to the present time n, all while respecting the observations z^n at time n. This feature of the importance function explains why the mean μ_j^n is written with the unusual notation (for perturbed observations) to include the deterministic model forecast from the previous time step. In summary, the weights of the EnKF are

$$w^n_{j,\ \mathrm{EnKF}} \propto w^{n-1}_{j,\ \mathrm{EnKF}} \ \frac{p(x_j^n|x_j^{n-1}) p(z^n|x_j^n)}{\pi^n_{j,\ \mathrm{EnKF}}(x^n|x_j^{n-1}, z^n)}.$$

Note that the *weighted* EnKF ensemble members are samples from the joint posterior (3), whereas the *unweighted* samples of the EnKF are samples of the (approximate) marginal posterior (4), i.e. the weights transform samples of the marginal posterior (4) into samples of the joint posterior (3). Thus, the collection of EnKF ensembles up to time n, viewed as a sample of the joint posterior from time 0 to time n, receives weights even when the data assimilation problem is linear and Gaussian. The reason is that the EnKF ensemble is not drawn from the joint posterior, but rather samples of the joint posterior are constructed sequentially by sampling the marginal posteriors at each step. If we analyze properties of the weights above then we are assessing how close or far one is from the joint posterior. In practice, one must be certain that this is the appropriate way to measure the quality of our data assimilation methodology. Below we neglect this question and present the standard theory [5, 7, 36, 37] to analyze these weights of the *joint posterior*. The

analysis has been done with particle filters before. Here we analyze EnKF's ability to approximate the *joint posterior*.

Using the results of [5, 7, 36, 37], the negative logarithm of the variance of the above weights governs the collapse of the EnKF (see also the review of particle filters above). Thus,

$$var(\gamma^n_{\text{EnKF}}) < \infty, \quad \text{as } m \to \infty, \tag{21}$$

where

$$\gamma^n_{\text{EnKF}} = -\log\left(\frac{p(x^n_j|x^{n-1}_j)p(z^n|x^n_j)}{\pi^n_{j,\ \text{EnKF}}(x^n|x^{n-1}_j, z^n)}\right),$$

is a condition for success with the EnKF for large dimensional problems (as a sequential sampler of the joint posterior). The main point of condition (21) is that it describes the collapse of EnKF in the same sense as the collapse of particle filters is described in [5, 7, 36, 37]. We thus examine this condition in detail.

For linear Gaussian problems (21) can be simplified as follows. With an optimal localization and inflation (or, equivalently, with a large but finite number of members) we can assume that the EnKF ensemble members are direct draws from the *marginal posterior* $p(x^n|z^{1:n})$. Under these assumptions, the EnKF importance function is

$$x^n_j \sim \pi(x^n|x^n_j, z^n) = p(x^n|z^{1:n}) = \mathcal{N}(\mu^n, P_n),$$

where μ^n is the mean of the marginal posterior, and the EnKF weights become

$$w^n \propto w^{n-1}\frac{p(x^n|x^{n-1})}{p(x^n|z^{1:n-1})}. \tag{22}$$

The denominator of the weights in (22) can be evaluated using

$$p(x^n|z^{1:n-1}) = \int p(x^n|x^{n-1})p(x^{n-1}|z^{1:n-1})dx^{n-1},$$

which, for the linear Gaussian problems we consider, is Gaussian:

$$p(x^n|z^{1:n-1}) = \mathcal{N}(A\mu^{n-1}, APA^T + Q).$$

The numerator in (22) can be read off of the model equation (1)

$$p(x^n|x^{n-1}) = \mathcal{N}(Ax^{n-1}, Q).$$

Thus,

$$\begin{aligned}\gamma^n_{\text{EnKF}} =& \frac{1}{2}\left(x^n - Ax^{n-1}\right)^T Q^{-1}\left(x^n - Ax^{n-1}\right), \\ &- \frac{1}{2}\left(x^n - A\mu^{n-1}\right)^T (APA^T + Q)^{-1}\left(x^n - A\mu^{n-1}\right),\end{aligned} \tag{23}$$

where $x^n = Ax^{n-1} + d^n$ and $x^{n-1} \sim \mathcal{N}(\mu^{n-1}, P)$. In general, the variance of γ^n_{EnKF} is not easy to analyze due to correlations in x^n and x^{n-1} (even in the linear/Gaussian case). However, we can illustrate the above condition for success with the EnKF (as a sequential sampler for the joint pdf) on the example used in [5,7,11,36,37]. Here the example is used to show that the limitations of the EnKF for sampling the joint posterior can be more severe than the limitations of particle filters.

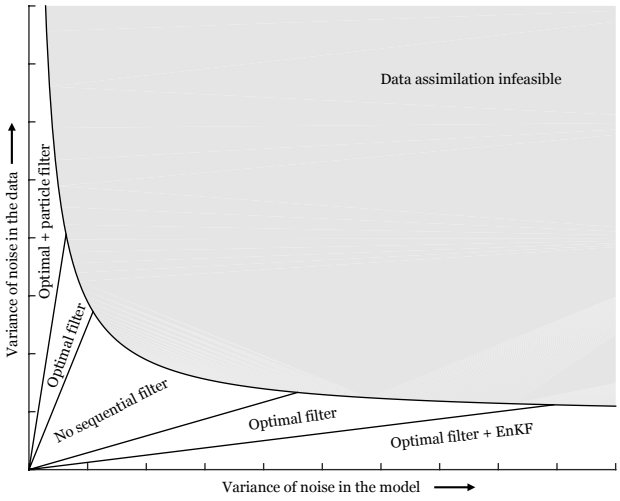

Figure 3: Conditions for feasible data assimilation and for successful sampling of the joint posterior with the optimal particle filter, the particle filter and EnKF.

3.1 Uncorrelated linear Gaussian example

We revisit the linear Gaussian example of section 2.3 (see (16) and [5,7,11,36,37]). For this example, the condition (21) for successful estimation of the joint posterior (3) with the EnKF becomes

$$\gamma^n_{\mathrm{EnKF}} = \frac{1}{2q}\sum_{j=1}^{m}(x_j^n - x_j^{n-1})^2 - \frac{1}{2(p+q)}\sum_{j=1}^{k}(x_j^{n-1} - \mu_j^{n-1})^2,$$

where p is as in (17). A calculation (see Appendix) shows that

$$var(\gamma^n_{\mathrm{EnKF}}) = m\frac{p}{p+q}. \tag{24}$$

The successful estimation of the *joint* posterior with the EnKF requires that $var(\gamma^n_{\mathrm{EnKF}}) = \mathrm{Const.}$ as $m \to \infty$ and, as before, we can set this constant to one (where, again, the number one is a proxy for a variance below which we believe that data assimilation is feasible) to find that

$$r \leq \frac{m}{(m-1)^2}q,$$

defines the condition for success with EnKF for sampling the joint posterior. The condition is illustrated in figure 3. We find that, for a fixed noise in the observations (fixed r), the EnKF can successfully sample the joint posterior only if the variance of the noise in the model is beyond a certain threshold. Because this condition is counter-intuitive we will return to discuss it shortly.

However, first we compare the conditions for success with the EnKF with the conditions for success with the optimal particle filter [16, 31, 44]. The optimal particle filter makes use of the optimal importance function

$$\pi^n_{\mathrm{j,\ opt}}(x^n; x_j^{0:n-1}, z^{1:n}) = p(x^n|x^{n-1}, z^n),$$

and its weights are

$$w^n_{\mathrm{opt}} \propto w^{n-1}_{\mathrm{opt}} p(z^n|x^{n-1}).$$

For our example, the condition for success with the optimal particle filter is

$$\left(m - \sqrt{2m} - \sqrt{m^2 - 2\sqrt{2}m^{1.5} - 6m}\right) q \leq 4(r+1) \leq \left(m - \sqrt{2m} + \sqrt{m^2 - 2\sqrt{2}m^{1.5} - 6m}\right) q, \tag{25}$$

(see [11], the calculation is also summarized in the appendix). The condition is illustrated in figure 3. We find that the optimal particle filter can be successful in two regimes: if the noise in the model is small (small q), then the noise in the observations can be large (large r), and if the noise in the observations is small (small r), then the noise in the model may be large (large q). This is in contrast to the condition for success with the EnKF, which requires accurate observations (small r), and a moderate noise in the model (moderate q). Thus, for this example, the optimal particle filter can be successful in situations in which the EnKF collapses.

This is perhaps not surprising, because our calculations simply confirm that the optimal particle filter is optimal. The reason is that its weights depend only on the state of the particles at time $n-1$, and no additional variance is introduced at the current step. Thus, the collapse of the optimal particle filter follows from the sequential approach to the data assimilation problem, i.e. from the factorization of the importance function as in (9). The collapse can only be avoided if present observations are used to inform past state estimates (i.e. if a broader family of importance functions is considered). We remind the reader that our conditions for success with particle filters are independent of practical considerations related to, e.g. the numerical cost of each sample.

Next, we compare the conditions for success with EnKF or the optimal particle filter with the conditions for success with the "standard" particle filter [15, 20] (we will refer to this standard particle filter as just a "particle filter" from now on). The particle filter uses the importance function (9) with

$$\pi^n_{j,\mathrm{PF}} = p(x^n | x^{n-1}_j),$$

so that its weights are

$$w^n_{j,\mathrm{PF}} \propto w^{n-1}_{j,\mathrm{PF}}\, p(z^n | x^n_j).$$

The condition for the particle filter to be successful is that $var(\gamma^n_{\mathrm{PF}}) = \text{Const.}$ as $m \to \infty$, where

$$\gamma^n_{\mathrm{PF}} = -\log\left(p(z^n | x^n_j)\right).$$

For the uncorrelated linear Gaussian problem we consider, this condition can be rearranged to (see appendix and [5, 7, 11, 37]):

$$r \geq \frac{1}{2}\left(m + \sqrt{2m}\right) q. \tag{26}$$

This condition is also illustrated in figure 3 and shows that the particle filter can only be successful if the noise in the model (q) is small compared to the noise in the observations (r).

In summary, the example shows that the EnKF and the particle filter may collapse in problems in which the optimal particle filter can be successful, i.e. the limitations of the EnKF, as a sequential sampler of the joint posterior, can be more severe than the limitations of optimal particle filters. Our results also show that EnKF collapses in the same way as other particle filters, when it is applied to the examples in [5, 7, 36, 37], which correspond to our example with $q = r = 1$.

Finally, we wish to discuss several remarkable and surprising features of our analysis. Recall that, for a fixed intensity of the noise in the observations (fixed r), the EnKF can be successful only if the intensity of the noise in the model (q) is beyond a certain threshold. However, one can think of decreasing the variance of the noise in the model (q) as improving the quality of the model. Our results thus indicate that the EnKF performs worse when the model is improved. The reason for this surprising behavior is as follows. To update the state trajectory from time $n-1$ to time n with

the EnKF, we sample the marginal (4), which, for this example, is a Gaussian with covariance given by (17). This covariance goes to 0 for fixed r and $q \to 0$. While it is true that the target density (joint posterior) also goes to zero in this limit it would appear that the marginal goes to zero faster. Thus, for a fixed r and smaller q, the covariance of the importance function underestimates the covariance of the target, which is the joint posterior, so that sampling of the joint posterior via the EnKF algorithm becomes inefficient because its particles are too close together. This also implies that we may not simply take the $q \to 0$ limit of all the above equations to understand the behavior of the EnKF on data assimilation problems with a deterministic model ($Q = 0$).

Similarly, success with the optimal particle filter requires that, for a fixed accuracy of the observations (fixed r), the intensity of the noise in the model (q) is beyond a threshold. On the other hand, the optimal particle filter can also be successful if, for a fixed noise in the model (q), the noise in the observations (r) is beyond a certain threshold. Thus, as one improves the quality of the observations, while keeping the quality of the model fixed, or as one improves the model, while keeping the quality of the observations fixed, the problem becomes more difficult to solve with the optimal particle filter. These surprising behaviors are due to an under-/over-estimation of the covariances in the optimal importance function. For the example we consider, the optimal importance function is Gaussian with variance $qr/(q+r)I_m$. Thus, the covariance of the optimal importance function goes to zero independently of q (or r) if $r \to 0$ (or $q \to 0$), so that, when both q and r are small, the covariance of the required update of the joint posterior is underestimated, which again can make the optimal particle filter inefficient as its particles are therefore too close together.

4 Efficiency of EnKF on marginal posteriors

The collapse of the EnKF on the joint posterior (described above) does not imply its collapse on the marginal posterior. Here we investigate the possible collapse of EnKF on the *marginal posterior*. The analysis requires weights of EnKF for the marginal posterior. We derive these weights separately for linear and nonlinear problems. To the best of our knowledge, these weights have not been reported before. We can prove optimality of an idealized EnKF (with optimal localization and inflation) for linear Gaussian problems, however can not claim optimality of EnKF for the marginal posterior of nonlinear problems, because the calculation of the weights is difficult and, in general, requires approximation.

4.1 Optimality of EnKF for the marginal posterior of linear problems

For linear/Gaussian problems, we can assume that a properly localized and inflated EnKF draws samples directly from the marginal posterior (see above). Recall that the weights are defined as the ratio of the distribution we wish to sample, the target density, and the density we use to generate the samples, the importance function. We emphasize that the target density is now the *marginal posterior*, and not the joint posterior as above. Because EnKF with localization and inflation draws samples from the marginal posterior, the target density and importance function are equal, so that the weights are constant. Said another way, the samples are perfect samples of the marginal posterior and therefore different ensemble members will not receive weights that differ from each other, i.e. the members are equally likely. Since the weights are constant, their variance is zero and the (localized and inflated) EnKF is an *optimal sampling algorithm for the marginal posterior of linear Gaussian problems*. Moreover, the EnKF never collapses (because collapse is defined as a non-zero variance of the weights) on the marginal posterior of (feasible) linear Gaussian data assimilation problems.

4.2 Weights of EnKF for the marginal posterior of nonlinear problems

For nonlinear problems, the EnKF ensemble must receive non-constant weights because it cannot properly produce samples from a non-Gaussian marginal posterior. In fact, various difficulties EnKF can run into when it attempts to produce samples from a non-Gaussian marginal posterior are described in [21, 22]. The weights are, as in the linear case, the ratio of the target density (the marginal posterior) and the importance function defined by EnKF:

$$w \propto \frac{p(z^n|x^n)p(x^n|z^{1:n-1})}{\pi_{\text{EnKF}}(x^n)}.$$

A basic requirement for weighted sampling (and many other sampling schemes, e.g. Markov Chain Monte Carlo) is that the target density and importance function be known up to a multiplicative constant. This is not the case here. The first term in the numerator, $p(z^n|x^n)$, is easy to evaluate, however the second, $p(x^n|z^{1:n-1})$ is, in general, not. If the problem is linear and Gaussian, we can write

$$p(x^n|z^{1:n-1}) = \int p(x^n|x^{n-1})p(x^{n-1}|z^{1:n-1})dx^{n-1}, \tag{27}$$

and evaluate this integral analytically (see section 3). However, for nonlinear problems, evaluation of this integral is difficult so that, in general, the target density is not known up to a multiplicative constant. Exact weights for EnKF for the marginal posterior are thus out of reach.

However, we can develop approximate weights by approximating the integral (27) using Monte Carlo methods. This approximation becomes exact as the ensemble size M goes to infinity. Let $x_j^{n-1} \sim p(x^{n-1}|z^{1:n-1})$, $j = 1, \ldots, M$, be the analysis ensemble at time $n-1$. This ensemble defines the approximation

$$p(x^{n-1}|z^{1:n-1}) \approx \frac{1}{M}\sum_{j=1}^{M} \delta(x^{n-1} - x_j^{n-1}), \tag{28}$$

which can be used in the integral (27) to obtain

$$p(x^n|z^{1:n-1}) \approx \frac{1}{M}\sum_{j=1}^{M} p(x^n|x_j^{n-1}).$$

The target density can thus be approximated by

$$p(x^n|z^{1:n}) \approx p(z^n|x^n)\left(\frac{1}{M}\sum_{j=1}^{M} p(x^n|x_j^{n-1})\right). \tag{29}$$

The probability of the analysis ensemble at time n given the analysis ensemble at time $n-1$ is known. It is the Gaussian given in (20). The marginal posterior weights however require the probability of the analysis ensemble at time n (without conditioning). This probability can be obtained by integrating the conditioned probability:

$$\pi_{\text{EnKF}}(x^n) = \int \pi^n_{\text{EnKF}}(x^n|x^{n-1}, z^n)p(x^{n-1}|z^{1:n-1})dx^{n-1}, \tag{30}$$

where $\pi^n_{\text{EnKF}}(x^n|x^{n-1}, z^n)$ is given in (20). Using (28), the importance function defined by EnKF can thus be approximated by :

$$\pi_{\text{EnKF}}(x^n) \approx \frac{1}{M}\sum_{j=1}^{M} \pi_{\text{EnKF}}(x^n|x_j^{n-1}, z^n).$$

With these approximations, the weights with respect to the marginal posterior are

$$w_{\text{EnKF}} \approx \hat{w}_{\text{EnKF}} \propto \frac{p(z^n|x^n)\sum_{j=1}^{M} p(x^n|x_j^{n-1})}{\sum_{j=1}^{M} \pi_{\text{EnKF}}(x^n|x_j^{n-1}, z^n)}. \tag{31}$$

The weights and their approximation are difficult to analyze in general. We study these weights with numerical experiments in section 5 below, and compare the marginal posterior weights with the joint posterior weights of section 3.

Finally, we want to report that the (approximate) weights for the marginal posterior are difficult to compute unless the model's time-stepper is in sync with the observations. The difficulties can be illustrated assuming that there is one additional model step between two consecutive observations. In this case, the importance density can be written as

$$\pi_{\text{EnKF}}(x^n) = \int\int \pi^n_{\text{EnKF}}(x^n|x^{n-1}, z^n) p(x^{n-1}|x^{n-2}) p(x^{n-2}|z^{1:n-2}) dx^{n-1} dx^{n-2}.$$

We can use the analysis ensemble at time $n-2$ to approximate $p(x^{n-2}|z^{1:n-2})$ as before, however we then must perform the integration over x^{n-1} (assuming there is no observation available at that time):

$$\pi_{\text{EnKF}}(x^n) \approx \frac{1}{M}\sum_{j=1}^{M} \int \pi^n_{\text{EnKF}}(x^n|x^{n-1}, z^n) p(x^{n-1}|x_j^{n-2}) dx^{n-1}.$$

This integration is difficult in general, which complicates the computation of the weights for EnKF (with respect to the marginal posterior). The above finding makes the weights impractical.

5 Illustration of the collapse with the stochastic Lorenz '63 model

In this section we will provide an explicit example of the collapse of the EnKF on the joint posterior. We also illustrate the use of the weights as well as the difference between the weights for the marginal and joint posteriors with numerical experiments with a stochastic version of the Lorenz '63 equations [32]:

$$\begin{aligned} dx_1 &= (\sigma(x_2 - x_1))\, dt + q\, dW_1, \\ dx_2 &= (x_1(\rho - x_3) - x_2)\, dt + q\, dW_2, \\ dx_3 &= (x_1 x_2 - \beta x_3)\, dt + q\, dW_3. \end{aligned}$$

Here $\rho = 28$, $\sigma = 10$, $\beta = 8/3$, W_1, W_2, W_3 are independent Brownian motions, and $q = \sqrt{2}$. The equations are discretized using a 4^{th}-order Runge-Kutta for the deterministic part and a forward Euler step for the Brownian motion. The time-step is $\Delta t = 5 \cdot 10^{-3}$. At each step of the discrete model, we collect observations of the states x and z, perturbed by independent Gaussian noise with standard deviation one. The initial conditions are Gaussian with mean $x_0 = (3.6314, 6.6136, 10.6044)^T$ and covariance matrix $P_0 = \text{diag}\,[(1, 3, 5)]$ (here $\text{diag}\,[a]$ is an $n \times n$ diagonal matrix whose diagonal elements are the components of the n-vector a).

We implement the EnKF with perturbed observations as described above, however we do not implement localization or inflation. Instead, we consider large enough ensembles (large compared to the state dimension) such that localization and inflation are not necessary (this can be done here only because the Lorenz '63 equations are low-dimensional). For comparison, we also implement the optimal particle filter which, for the set-up we consider, coincides with the implicit particle filter [4, 12, 13, 33].

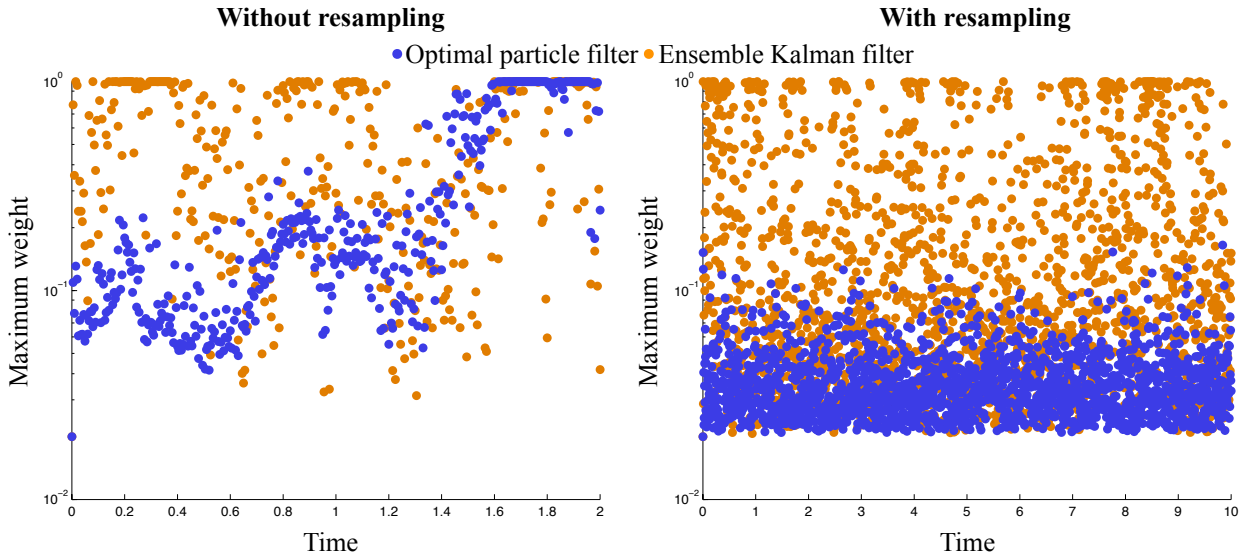

Figure 4: Maximum weight of the EnKF (weighted with respect to the joint posterior) and of the optimal particle filter as a function of time. Left: both algorithms are implemented without resampling. Right: both algorithms are implemented with resampling.

5.1 The collapse on the joint posterior

We first consider the EnKF weighted with respect to the joint posterior as described in section 3 and perform numerical experiments with synthetic data. We run the discrete model for ten dimensionless time units and collect observations perturbed by the appropriate noise. These observations are the input to the weighted EnKF. We first consider an implementation *without* resampling. At each assimilation, we compute the weights and store the maximum weight. If this maximum weight equals one, the filter has collapsed. In the left panel of figure 4, we plot the maximum weight of the EnKF with 50 ensemble members as a function of time and find that the EnKF collapses immediately. The maximum weight of the optimal particle filter with 50 samples is also shown in the left panel of figure 4. We find that the optimal particle filter collapses after a few hundred steps (after about 1.5 dimensionless time units). The reason is that the variance of the negative logarithm of the weights of the optimal particle filter is reduced compared to the EnKF, which delays the collapse (but does not prevent it).

For this example, the collapse can be prevented by resampling. In resampling, one replaces samples with a low weight with samples with a high weight without introducing significant bias [15]. The maximum weights of the EnKF and optimal particle filter with resampling (after each assimilation) are plotted as a function of time in the right panel of figure 4. We find that the maximum weight of the optimal particle filter is never larger than about 0.3, however the EnKF collapses on the joint posterior even with frequent resampling. This example illustrates that EnKF may be a suboptimal choice if the posterior probability of interest is the joint posterior (3).

5.2 The non-collapse on the marginal posterior

We consider the EnKF weighted with respect to the marginal posterior as explained in section 4. The weights are approximated with equation (31). As before, we run numerical experiments with synthetic data and with the same parameters as above. At each assimilation, we compute the

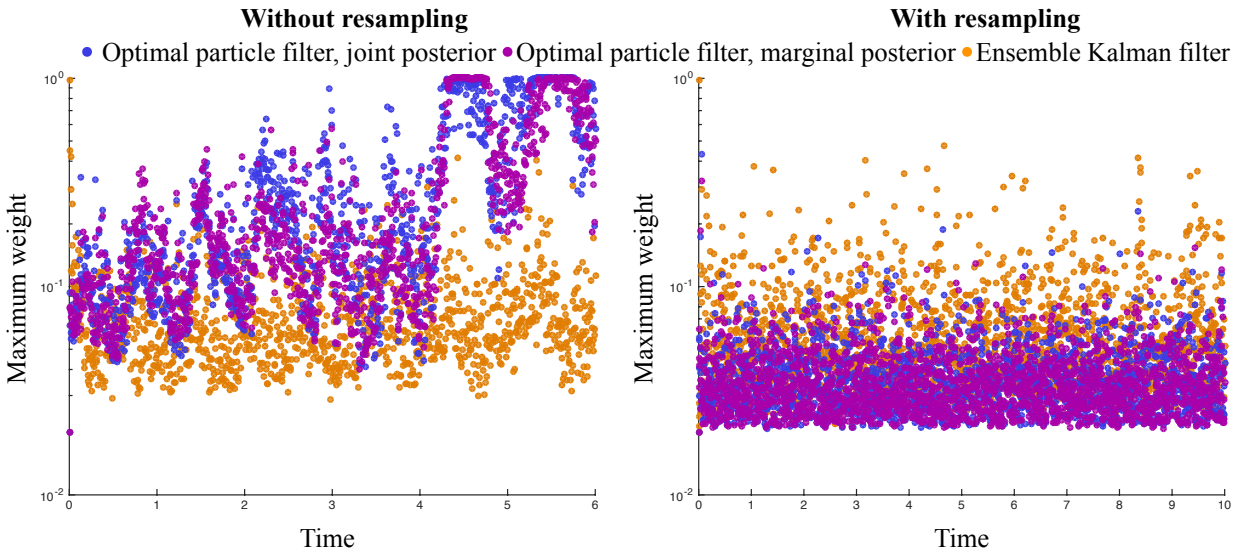

Figure 5: Maximum weight of the EnKF (weighted with respect to the marginal posterior) and of the optimal particle filter (weighted with respect to the joint or marginal posterior) as a function of time. Left: all three algorithms are implemented without resampling. Right: all three algorithms are implemented with resampling.

weights of the 50 EnKF ensemble members with respect to the marginal posterior. The results are shown in figure 5. We find that the maximum weight of the EnKF is not so close to one as to indicate a collapse. Moreover, a resampling strategy, which is necessary to avoid the collapse of the optimal particle filter, is not needed for the EnKF (see left panel of figure 5). However, resampling can improve the quality of the ensemble, as measured by the maximum weight. In the right panel of figure 5, we plot the maximum weight of EnKF with resampling after each step, to illustrate that the maximum weight of EnKF is reduced by the resampling. Specifically, the mean of the maximum weight was reduced from 0.076 to 0.066.

We compare the weighted EnKF ensemble with the samples of the optimal particle filter. Recall that the optimal particle filter generates weighted samples of the joint posterior (3). These samples can be marginalized by simply dropping their past. As described in the previous section, the optimal particle filter collapses (i.e. its maximum weight is one), unless a resampling strategy is used (see left panel of figure 5). However, with resampling, the maximum weight of the optimal particle filter is often less than the maximum weight of the weighted EnKF (see right panel of figure 5), indicating that the samples of the optimal particle filter are well distributed with respect to the joint posterior. This may not be the case in other examples, in which the optimal particle filter collapses (see figure 3).

In such cases, one can re-weight the samples of the optimal particle filter directly with respect to the joint posterior. This idea is explained for the (standard) particle filter in [29]. Here, we briefly discuss how to marginalize the optimal particle filter. It is important to understand that this filter is not "optimal" as a sampler for the marginal posterior. We derive the weights with respect to the marginal posterior for the optimal particle filter in the same way as for the EnKF, and use the approximation (29) for the target density. To find the importance function, we integrate over the

samples at time $n-1$ as above,

$$\pi_{\text{opt}}(x^n) = \int \pi^n_{\text{opt}}(x^n|x^{n-1}, z^n) p(x^{n-1}|z^{1:n-1}) dx^{n-1},$$

and approximate $p(x^{n-1}|z^{1:n-1})$ with the sum of delta distributions (28) to find

$$\pi_{\text{opt}}(x^n) \approx \frac{1}{M} \sum_{j=1}^{M} \pi^n_{\text{opt}}(x^n|x^{n-1}_j, z^n).$$

With these approximations, the weights with respect to the marginal posterior become

$$w_{\text{opt}} \approx \hat{w}_{\text{opt}} \propto \frac{p(z^n|x^n) \sum_{j=1}^{M} p(x^n|x^{n-1}_j)}{\sum_{j=1}^{M} \pi^n_{\text{opt}}(x^n|x^{n-1}_j, z^n)}.$$

This re-weighted optimal particle filter is also applied to the Lorenz '63 equations, and the maximum weight is plotted as a function of time in figure 5. The optimal filter, weighted with respect to the marginal posterior, collapses unless a resampling strategy is implemented (see left panel of figure 5). However, with resampling, the optimal filter weighted with respect to the marginal posterior has, on average, the smallest maximum weight. The improvement compared to the optimal particle filter is not too large, since the optimal particle filter produces samples that are well distributed with respect to the posterior. The direct re-weighing of its samples in this example leads to a minor improvement of the distribution of the samples with respect to the marginal posterior. For example the mean of the maximum weight of the optimal particle filter is 0.37, and the mean of the maximum weight of the optimal particle filter weighted with respect to the marginal is 0.36.

6 Connections to mean square error and previous work

Previous work on the scaling of EnKF's required ensemble size includes [19], where a rigorous analysis of forecast and posterior sample covariance matrices is presented. The analysis in [19] suggests that the ensemble size of the EnKF must scale quadratically with the state dimension to keep the sampling error bounded. If this were true, then the EnKF would be impractical for geophysical applications (where the state dimension usually exceeds 10^6). Nonetheless, the EnKF appears to perform adequately in many geophysical applications.

We wish to understand this contradiction better using the methods presented here and the theory of feasible data assimilation. To investigate these issues, the "error" in the EnKF state estimate is often described by the mean square error (MSE) defined as

$$\text{MSE} = \frac{1}{m} \sum_{i=1}^{m} \left((\bar{x}^n)_i - (x^t)_i \right)^2, \tag{32}$$

where x^t is the "true" state of the model and $(x^t)_i$, $i = 1, \ldots m$ are its m components, and where

$$\bar{x}^n = \frac{1}{M} \sum_{j=1}^{M} x^n_j,$$

is the sample mean at time n, computed from the EnKF analysis ensemble members x^n_j, $j = 1, \ldots, M$. We further define an error in the sample covariance by the Frobenius norm squared of the difference of the sample covariance in (5) and the true marginal posterior covariance

$$\text{SCE} = ||X_n - P_n||^2_F. \tag{33}$$

This definition is in line with [19], where a similar error measure is used. We wish to find out how the above errors scale with the dimension m and EnKF sample size, M, and study this scaling using the linear Gaussian example of section 2.3 (see also equation (16 and [5, 7, 11, 36, 37]).

If the EnKF is localized and inflated in such a way that its samples are direct draws from the marginal posterior (as before), then one can use the central limit theorem to compute the statistics of the MSE

$$\bar{x}^n \sim \mathcal{N}(\mu^n, \frac{p^n}{M} I_m).$$

Assuming that the true state is also a sample of the marginal posterior, one can combine the above expression for the sample mean with the expression (32) for the MSE and use the central limit theorem again to obtain the statistics of the MSE:

$$\text{MSE} \sim \mathcal{N}\left(p^n\left(\frac{M+1}{M}\right), 2\left(\frac{M+1}{M}\right)^2 \frac{(p^n)^2}{m}\right). \tag{34}$$

Thus, the ensemble size influences the MSE mildly through a factor $(M+1)/M$ (for example, with $M = 50$, $(M+1)/M = 1.02$). Moreover, the error in the MSE decreases quickly with the system dimension m. This means that, in a typical experiment, one finds an MSE of about p^n, and the standard deviation is $p^n/\sqrt{m}$, almost independently of the ensemble size M.

In [19], sampling error is measured by sampling errors in covariance matrices. We use a similar idea and measure sampling error in the covariance matrix by the SCE 33. To compute the statistics of SCE, we note that the sample covariance in (5) is Wishart distributed and, for the example we consider, the mean and variance (in each element) are

$$E(X_n) = p^n I_m, \quad var\left((X_n)_{i,j}\right) = \frac{1}{M} p^n. \tag{35}$$

Assuming that the elements of the sample covariance are uncorrelated (which we verify with numerical experiments below), one can use the central limit theorem to find that the error of the sample covariance (33) is Gaussian distributed:

$$\text{SCE} \sim \mathcal{N}\left((p^n)^2 \frac{m^2}{M}, 2\frac{(p^n)^4 m^2}{M}\right). \tag{36}$$

Thus, the ensemble size M must scale quadratically with the dimension m of the system if one requires that this error be bounded as the dimension goes to infinity (and assuming that p^n is order 1). This result agrees with what was found by a similar analysis of the forecast and analysis covariance matrices in [19]. Thus, we showed that:

1. the MSE may not be a good indicator for the required size of the EnKF ensemble because its statistics are insensitive to the ensemble size;

2. a bounded error in the sample covariance (SCE) requires a quadratic scaling of the ensemble size with the dimension of the problem.

The second statement however does not agree with what is found in practice, where EnKFs perform "well" with small ensemble sizes on high-dimensional problems. The reason is a feasibility of data assimilation, as described in [11] and reviewed in section 2.3 above. Recall that bounded feasible data assimilation requires that

$$p \propto \frac{1}{\sqrt{m}}. \tag{37}$$

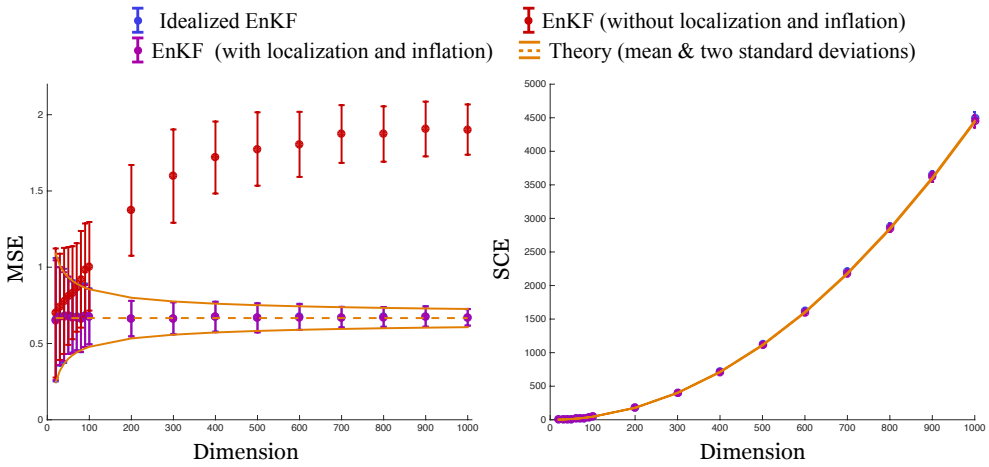

Figure 6: Scaling of MSE and SCE with system dimension.

With this scaling, EnKF requires an ensemble whose size scales *linearly* with the dimension of the problem. If the effective dimension is even smaller, e.g. $p \propto 1/m$, then even smaller ensemble sizes may give accurate results (in terms of the error in the sample covariance).

We illustrate the above (asymptotic) results with numerical experiments and confirm that EnKF (with localization and inflation) can give bounded errors in the sample covariance in large-dimensional systems, even if the ensemble size is small. We implement an EnKF without localization or inflation, one with diagonal localization and an adaptive, multiplicative inflation with a factor $(1+1/M)$. We also implement the "idealized" EnKF (used in the analysis above) in which we draw samples directly from the marginal posterior. We vary the dimension of the problem from $m = 10$ to $m = 1000$ and, for a fixed m, we draw a "true" state from the marginal posterior, generate a synthetic datum (by adding the appropriate noise to the true state), and run all three EnKFs to compute their MSE and SCE. We do this 100 times for each m to demonstrate and illustrate the scaling of the mean and standard deviation of the MSE and SCE with the dimension m of the problem.

6.1 Numerical experiments with an infeasible data assimilation problem

We first consider the example of section 2.3 with equally strong noises in the model, i.e. we set $q = r = 1$ and $n = 1$ (this is the same example as in [5, 7, 36, 37]). We further assume that $x^0 \sim \mathcal{N}(0, I_m)$ so that $p^1 = 2/3$. We plot the results of 100 numerical experiments in figure 6. For the experiments, we use a constant ensemble size of $M = 100$. The left panel of figure 6 shows the scaling of the MSE with the dimension m and the right panel shows the scaling of the sample covariance error.

We find that our theory in equations (34) and (36) correctly predicts the numerical results: the MSE remains constant with the dimension m of the system and, for a fixed ensemble size, the SCE (36) scales quadratically with the problem dimension. Moreover, our assumption that a localized and inflated EnKF produces direct samples from the marginal posterior (in linear problems) is confirmed by the experiments, since the MSE/SCE statistics we compute with the idealized EnKF agree with those computed with the localized/inflated EnKF.

The example also underlines the importance of localization and inflation. The vanilla EnKF (without localization and inflation) yields a much larger MSE than the inflated/localized EnKF.

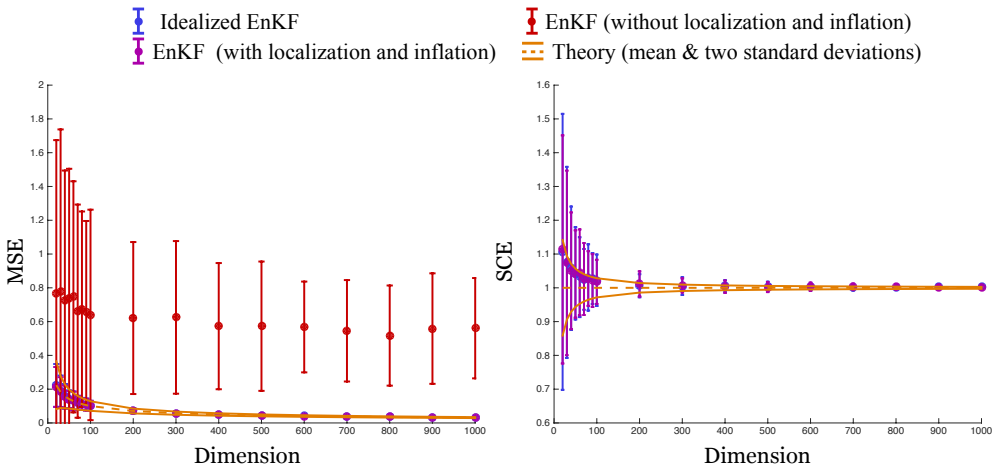

Figure 7: Scaling of error in sample covariance with system dimension for a feasible problem.

While the MSE may be insensitive to the ensemble size, it can be sensitive to localization and inflation and, thus, the MSE may be used to efficiently "tune" the localization and inflation.

6.2 Numerical experiments with a feasible data assimilation problem

We now assume a problem as in section 2.3, but with noises in model and data that lead to a feasible problem, i.e. we assume that the balance condition (19) is satisfied. As before, we vary the state dimension m, however also vary q and r with m such that (19) holds, and set the ensemble size equal to the state dimension, i.e. $M = m$. The changes in q and r can be linked to the geophysically relevant problem of fixing r and reducing q as the state dimension increases (i.e. as the grid is refined) because we assume that the model converges with increases in resolution. The results of 100 experiments are shown in figure 7. As before, we find that the results for the idealized EnKF and the localized/inflated EnKF overlap, which once more confirms our assumptions about localization and inflation above. Moreover, the results confirm the theory we developed: in a feasible problem, an ensemble size that scales linearly with the state dimension, leads to constant errors in the sample covariance (SCE) as the dimension of the problem increases. Figure 7 also illustrates the effects and validity of our assumption that the elements of the sample covariance are uncorrelated. For small m, the ensemble size is small and the assumption is violated. However, for large m, the ensemble size M is large enough such that our assumption is a valid approximation.

6.3 Discussion and meteorological interoperation of our results

Whether geophysically relevant problems are feasible or infeasible remains an open question. The behavior of the example in figure 6, where the localized and unlocalized EnKF have smaller MSE for larger state dimensions, is not seen in practice. The reason may be that the theory of feasible data assimilation works best if the model is a PDE on a mesh and that the mesh has been refined to the point of convergence. This has not occurred yet for the typical resolutions of global meteorological models. In meteorology, the typical behavior seen in the EnKF is more like figure 7, for which data assimilation is labeled infeasible by our theory and where increases in resolution lead to harder and harder problems to solve.

One can sensibly break meteorological data assimilation into two cases: tropics and mid-latitudes. In the tropics, where convective processes and small-scale waves dominate the dynamics,

the correlation length scales are small relative to the typical grid resolutions of global models. In this region, it is likely that global meteorological models are far from a mesh size that has converged. It is likely that, for a given observation error (fixed r), the model error (q) may not decrease fast enough as the mesh is refined so that data assimilation in the tropics remains difficult. If the resolution were to increase to the point that these convective systems and tropical waves were resolved, then further refinements of the grid beyond this point would lead to a more rapidly decreasing q and, therefore, to a feasible data assimilation problem. By contrast, in mid-latitudes, where significantly larger scale waves dominate the dynamics, one might presume that the resolution of the model is sufficient to resolve the dominant processes. However, if this were the case we would see the EnKF behave as in figure 7 such that increases in resolution would result in reductions in MSE. However, this behavior is not observed in practice, which indicates that even at mid-latitudes the mesh size is still too large to assess wether or not the problem as feasible. Further study of the relationship between feasibility and geophysical data assimilation is required here.

Our analysis also shows that the MSE is not a robust and reliable indicator for the EnKF to "be working". The statistics of the MSE (see above) show that MSE is insensitive to the ensemble size. In fact, one may observe large sampling error (in the covariance, even after localization), even though the MSE is "small". Thus, tuning of EnKF based on MSE may be uninformative regarding the statistics of the EnKF ensemble.

However, these results rely on our assumptions being valid. In particular, we assume that the data assimilation problem be linear and Gaussian and that the (localized and inflated) EnKF produces samples from the marginal posterior. Our analysis assesses the performance of EnKF ensembles with this property. However, in linear or nonlinear problems, sampling error in the EnKF may produce a bias in the ensemble's estimate of the posterior variance [35]. This bias in the ensemble's estimate of the posterior variance is one of the features one accounts for with typical prior/posterior inflation methods. If the inflation method worked perfectly, then we may assume that the EnKF produces an ensemble variance that is not biased as in equation 35. The results of our analysis then shows that the MSE is only a weak function of the ensemble variance (under the above assumptions). This implies that the typical tuning regimen of attempting to match the posterior MSE to the posterior variance is a method to adjust the posterior variance rather than a method for adjusting the error of the posterior mean.

7 Conclusions

We summarize our main results and repeat the assumptions under which the results are valid.

1. There are two posterior densities of interest in data assimilation. The *joint posterior* describes the probability of a state trajectory given the data and is the posterior usually considered in particle filtering. The *marginal posterior* describes the probability of the current state, given the data, and is the posterior usually considered in EnKF. For an accurate forecast (e.g. in numerical weather prediction) computation of the marginal posterior is sufficient.

2. The EnKF ensemble can be re-weighted with respect to the joint posterior or the marginal posterior. We have derived expressions for these weights and their approximation (in nonlinear cases).

3. Based on the weights for the *joint posterior*, we have shown that EnKF collapses in the same way as other particle filters and under even broader conditions and even for linear problems. However, the collapse of EnKF on the joint posterior does not imply its collapse on the marginal posterior.

4. The EnKF with localization and inflation is an optimal sampling algorithm for the *marginal posterior* of linear problems in the sense that the EnKF weights for the marginal posterior have minimum variance. The optimality for the marginal posterior of linear problems suggests that EnKF can work well for marginal posterior of mildly nonlinear problems. This explains the broad usefulness of EnKF in mildly nonlinear applications in which the marginal posterior is the probability of interest.

5. EnKF is a suboptimal choice for sampling the joint posterior, and particle filters are more broadly applicable to this problem.

6. Previous work on required ensemble sizes of EnKF suggests that the ensemble size must scale quadratically with the state dimension to keep the sampling error bounded. However this contradicts what is found in practice, where EnKF is reported to perform well on large-dimensional problems. We explained this contradiction by connecting EnKF to the theory of feasible data assimilation problems and we have shown with examples that the EnKF ensemble size can scale linearly (or slower) with the state dimension if the problem is feasible.

7. We have shown that the MSE may not be a reliable indicator for the quality of the EnKF ensemble. Specifically, the MSE may be "small" even though the sampling error is huge.

Acknowledgements

This material is based upon work supported by the U.S. Department of Energy, Office of Science, Office of Advanced Scientific Computing Research, Applied Mathematics program under contract DE-AC02005CH11231, and by the National Science Foundation under grant DMS-1217065. D. Hodyss gratefully acknowledges support from the Office of Naval Research PE-0601153N

Appendix

We provide details of some calculations.

Derivation of equation (24)

We wish to compute the variance of γ^n_{EnKF} in (24). For the linear Gaussian problems we consider, γ^n_{EnKF} is given by (23). Note that $x^n - Ax^{n-1} = d^n \sim \mathcal{N}(0, Q)$, so that (23) becomes

$$\gamma^n_{\text{EnKF}} = \frac{1}{2}\left(d^n\right)^T Q^{-1} d^n - \frac{1}{2}\left(d^n - A(\mu^{n-1} - x^{n-1})\right)^T \left(APA^T + Q\right)^{-1} \left(d^n - A(\mu^{n-1} - x^{n-1})\right).$$

Define

$$y^n = A(x^{n-1} - \mu^{n-1}),$$

and note that y^n and d^n are independent. With the above definition of y^n, γ^n_{EnKF} becomes

$$\gamma^n_{\text{EnKF}} = \frac{1}{2}\left(d^n\right)^T Q^{-1} d^n - \frac{1}{2}\left(d^n + y^n\right)^T \left(APA^T + Q\right)^{-1} \left(d^n + y^n\right)).$$

For the example defined by (16), the above expression simplifies to

$$\gamma^n_{\text{EnKF}} = \frac{1}{2q}\sum_{j=1}^{m}(d^n_j)^2 - \frac{1}{2p+q}\sum_{j=1}^{m}(d^n_j + y^n_j)^2,$$

where d_j^n and y_j^n are the components of d^n and y^n. Each term in the above sum simplifies to

$$\frac{d^2}{2q} - \frac{(d+y)^2}{2(p+q)} = \frac{pd^2 - qy^2}{2q(p+q)} - \frac{dy}{p+q},$$

where d and y denote one component of d^n and y^n. Its variance is

$$var\left(\frac{pd^2 - qy^2}{2q(p+q)} - \frac{dy}{p+q}\right) = var\left(\frac{pd^2 - qy^2}{2q(p+q)}\right) + var\left(\frac{dy}{p+q}\right) - 2cov\left(\frac{pd^2 - qy^2}{2q(p+q)}, \frac{dy}{p+q}\right).$$

Since $var(d^2) = 2q^2$ and $var(y^2) = 2p^2$, the variance of the first term is

$$var\left(\frac{pd^2 - qy^2}{2q(p+q)}\right) = \frac{p^2}{4q^2(p+q)^2}\, var(d^2) + \frac{q^2}{4q^2(p+q)^2} var(y^2) = \frac{p^2}{(p+q)^2}.$$

Recall that $E(d) = 0$, $E(d^2) = q$, $E(y) = 0$ and $E(y^2) = p$. The second term therefore is

$$var\left(\frac{dy}{p+q}\right) = \frac{1}{(p+q)^2}\left(E[d^2y^2] - E(yd)^2\right) = \frac{1}{(p+q)^2}\left(E(d^2)E(y^2)\right) = \frac{pq}{(p+q)^2}.$$

The covariance term is zero because y and d are mean zero and independent:

$$\begin{aligned} cov\left(\frac{pd^2 - qy^2}{2q(p+q)}, \frac{dy}{p+q}\right) &= E\left(\frac{pd^2 - qy^2}{2q(p+q)} \cdot \frac{dy}{p+q}\right) - E\left(\frac{pd^2 - qy^2}{2q(p+q)}\right) E\left(\frac{dy}{p+q}\right), \\ &= \frac{1}{2q(p+q)^2}\left(pE(yd^3) - qE(y^3d)\right) = 0. \end{aligned}$$

Thus,

$$var\left(\frac{pd^2 - qy^2}{2q(p+q)} - \frac{dy}{p+q}\right) = \frac{p^2}{(p+q)^2} + \frac{pq}{(p+q)^2} = \frac{p}{p+q}.$$

Adding up the m individual terms gives

$$\gamma_{\text{EnKF}}^n = m\frac{p}{p+q}.$$

Derivation of equation (25)

For a linear Gaussian data assimilation problem defined by (2) and (11),

$$p(z^n|x^{n-1}) \propto \exp\left(-\frac{1}{2}\left(z^n - Hx^{n-1}\right)^T \left(HQH^T + R\right)^{-1}\left(z^n - Hx^{n-1}\right)\right),$$

so that

$$\gamma_{\text{opt}}^n = -\frac{1}{2}\left(z^n - Hx^{n-1}\right)^T \left(HQH^T + R\right)^{-1}\left(z^n - Hx^{n-1}\right),$$

see also [11,36]. For our example, with A, H, Q and R as in (16),

$$\gamma_{\text{opt}}^n = -\frac{1}{2(q+r)}\sum_{j=1}^{m}\left(z_j^n - x_j^{n-1}\right)^2. \tag{38}$$

Define $u^n = z^n - x^n \sim \mathcal{N}(z^n - \mu^n, pI_m)$, and shift the origin such that $z^n - \mu^n = 0$ to obtain

$$\gamma_{\text{opt}}^n = \frac{1}{2(q+r)}\sum_{j=1}^{n}(u_j^n)^2,$$

where u_j^n are the components of u^n. These components are iid. Let $u \sim \mathcal{N}(0,p)$ denote one of the components and recall that $var(u^2) = 2p^2$ to find that

$$var(\gamma_{\text{opt}}^n) = m\frac{var(u^2)}{4(q+r)^2} = m\frac{p^2}{2(q+r)^2},$$

where, as before, $p = (q^2 + \sqrt{4qr} - q)/2$. The condition for success with the optimal filter is that $var(\gamma_{\text{opt}}^n) = \text{Const.}$ as $m \to \infty$. Setting this constant to one (as before) gives

$$\frac{p^2}{2(p+r)^2} < \frac{1}{m},$$

which can be rearranged to (25) by substituting the expression (17) for p.

Derivation of equation (26)

For the linear problem we consider,

$$\gamma_{\text{PF}} = -\log\left(p(z^n|x^n)\right) = \frac{1}{2r}\sum_{i=1}^{m}\left((y)_i - (x^n)_i\right)^2,$$

where, assuming that n is large enough such that the system has reached steady state, $x^n \sim \mathcal{N}(\mu^n, q+p)$. Define $(u)_i = (y-x)_i \sim \mathcal{N}((\bar{u})_i, (p+q)I_m)$, and shift the origin such that $(\bar{u})_i = 0$ for all $i = 1, \ldots, m$. Note that u_i are iid, so that

$$var\left(\gamma_{\text{PF}}\right) = m\frac{(p+q)^2}{2r^2}.$$

The condition for success with the particle filter is that $var\left(\gamma_{\text{PF}}\right) = \text{Const.}$ as $m \to \infty$. Setting the constant to one (as before) and rearranging gives (26).

References

[1] M. Ades and P.J. van Leeuwen. An exploration of the equivalent weights particle filter. *Quarterly Journal of the Royal Meteorological Society*, 139(672):820–840, 2013.

[2] J.L. Anderson. An ensemble adjustment kalman filter for data assimilation. *Monthly Weather Review*, 129:2884–2903, 2001.

[3] M.A. Arulampalam, S. Maskell, N.J. Gordon, and T. Clapp. A tutorial on particle filters for online nonlinear/non-Gaussian Bayesian tracking. *IEEE Transactions on Signal Processing*, 50(2):174–188, 2002.

[4] E. Atkins, M. Morzfeld, and A.J. Chorin. Implicit particle methods and their connection with variational data assimilation. *Monthly Weather Review*, 141:1786–1803, 2013.

[5] T. Bengtsson, P. Bickel, and B. Li. Curse of dimensionality revisited: the collapse of importance sampling in very large scale systems. *IMS Collections: Probability and Statistics: Essays in Honor of David A. Freedman*, 2:316–334, 2008.

[6] A.F. Bennet, L.M. Leslie, C.R. Hagelberg, and P.E. Powers. A cyclone prediction using a barotropic model initialized by a general inverse method. *Monthly Weather Review*, 121:1714–1728, 1993.

[7] P. Bickel, T. Bengtsson, and J. Anderson. Sharp failure rates for the bootstrap particle filter in high dimensions. *Pushing the Limits of Contemporary Statistics: Contributions in Honor of Jayanta K. Ghosh*, 3:318–329, 2008.

[8] C.H. Bishop, B.J. Etherton, and S.J. Majumdar. Adaptive sampling with the ensemble transform kalman filter. part i: Theoretical aspects. *Monthly Weather Review*, 129:420–436, 2001.

[9] M. Bocquet, C.A. Pires, and L. Wu. Beyond Gaussian statistical modeling in geophysical data assimilation. *Monthly Weather Review*, 138:2997–3023, 2010.

[10] A.J. Chorin and O.H. Hald. *Stochastic tools in mathematics and science*. Springer, third edition, 2013.

[11] A.J. Chorin and M. Morzfeld. Conditions for successful data assimilation. *Journal of Geophysical Research – Atmospheres*, 118:11,522–11,533, 2013.

[12] A.J. Chorin, M. Morzfeld, and X. Tu. Implicit particle filters for data assimilation. *Communications in Applied Mathematics and Computational Science*, 5(2):221–240, 2010.

[13] A.J. Chorin and X. Tu. Implicit sampling for particle filters. *Proceedings of the National Academy of Sciences*, 106(41):17249–17254, 2009.

[14] A. Doucet. On sequential Monte Carlo methods for Bayesian filtering. *Dept. Eng., Univ. Cambridge, UK, Techn. Rep.*, 1998.

[15] A. Doucet, N. de Freitas, and N. Gordon, editors. *Sequential Monte Carlo methods in practice*. Springer, 2001.

[16] A. Doucet, S. Godsill, and C. Andrieu. On sequential Monte Carlo sampling methods for Bayesian filtering. *Statistics and Computing*, 10:197–208, 2000.

[17] G. Evensen. *Data assimilation: the ensemble Kalman filter*. Springer, 2006.

[18] A. Fournier, G. Hulot, D. Jault, W. Kuang, W. Tangborn, N. Gillet, E. Canet, J. Aubert, and F. Lhuillier. An introduction to data assimilation and predictability in geomagnetism. *Space Science Review*, 155:247–291, 2010.

[19] R. Furrer and T. Bengtsson. Estimation of high-dimensional prior and posterior covariance matrices in kalman filter variants. *Journal of Multivariate Analysis*, 98:227–255, 2004.

[20] N.J. Gordon, D.J. Salmond, and A.F.M. Smith. Novel approach to nonlinear/non-Gaussian Bayesian state estimation. *Radar and Signal Processing, IEEE Proceedings F*, 140(2):107–113, 1993.

[21] D. Hodyss. Ensemble state estimation for nonlinear systems using polynomial expansions in the innovation. *Monthly Weather Review*, 139:3571–3588, 2011.

[22] D. Hodyss and W.F. Campbell. Square root and perturbed observation ensemble generation techniques in kalman and quadratic ensemble filtering algorithms. *Monthly Weather Review*, 141:2561–2573, 2013.

[23] D. Hodyss and N. Nichols. The error of representation: basic understanding. *Tellus A*, 67:24822, 2015.

[24] R.E. Kalman. A new approach to linear filtering and prediction theory. *Transactions of the ASME–Journal of Basic Engineering*, 82(Series D):35–48, 1960.

[25] R.E. Kalman and R.S. Bucy. New results in linear filtering and prediction theory. *ASME Journal of Basic Engineering, Series D*, 83:95–108, 1961.

[26] E. Kalnay. *Atmospheric Modeling, Data Assimilation, and Predictability.* Cambridge University Press, 2003.

[27] M.H. Kalos and P.A. Whitlock. *Monte Carlo methods*, volume 1. John Wiley & Sons, 1 edition, 1986.

[28] M. Khlalil, A. Sarkar, S. Adhikari, and D. Poirel. The estimation of time-invariant parameters of noisy nonlinear oscillatory systems. *Journal of Sound and Vibration*, 344:81–100, 2015.

[29] M. Klaas, N. de Freitas, and A. Doucet. Towards practical n2 monte carlo: The marginal particle filter. *Proceedings of the 21st Annual Conferebce on Uncertainty in Artificial Intelligence (UAI-05), Arlington, VA*, pages 308–315, 2005.

[30] P. Lancaster and L. Rodman. *Algebraic Riccati equations.* Oxford University Press, 1995.

[31] J.S. Liu and R. Chen. Blind deconvolution via sequential imputations. *Journal of the American Statistical Association*, 90(430):567–576, 1995.

[32] E.N. Lorenz. Deterministic nonperiodic flow. *Journal of the Atmospheric Sciences*, 20(2):130–141, 1963.

[33] M. Morzfeld, X. Tu, E. Atkins, and A.J. Chorin. A random map implementation of implicit filters. *Journal of Computational Physics*, 231:2049–2066, 2012.

[34] N. Papadakis, E. Memin, A. Cuzol, and N. Gengembre. Data assimilation with the weighted ensemble kalman filter. *Tellus*, 62A:673–697, 2010.

[35] W. Sacher and P. Bartello. Sampling errors in ensemble kalman filtering. part i: Theory. *Monthly Weather Review*, 136:3035–3049, 2008.

[36] C. Snyder. Particle filters, the "optimal" proposal and high-dimensional systems. *Proceedings of the ECMWF Seminar on Data Assimilation for Atmosphere and Ocean.*, 2011.

[37] C. Snyder, T. Bengtsson, P. Bickel, and J. Anderson. Obstacles to high-dimensional particle filtering. *Monthly Weather Review*, 136(12):4629–4640, 2008.

[38] O. Talagrand and P. Courtier. Variational assimilation of meteorological observations with the adjoint vorticity equation. I: Theory. *Quarterly Journal of the Royal Meteorological Society*, 113(478):1311–1328, 1987.

[39] M.K. Tippet, J.L. Anderson, C.H. Bishop, T.M. Hamill, and J.S. Whitaker. Ensemble square root filters. *Monthly Weather Review*, 131:1485–1490, 2003.

[40] P.J. van Leeuwen. Particle filtering in geophysical systems. *Monthly Weather Review*, 137:4089–4144, 2009.

[41] P.J. van Leeuwen. Nonlinear data assimilation in geosciences: an extremely efficient particle filter. *Quarterly Journal of the Royal Meteorological Society*, 136(653):1991–1999, 2010.

[42] E. Vanden-Eijnden and J. Weare. Data assimilation in the low noise regime with application to the Kuroshio. *Monthly Weather Review*, 141:1822–1841, 2012.

[43] J. Weare. Particle filtering with path sampling and an application to a bimodal ocean current model. *Journal of Computational Physics*, 228:4312–4331, 2009.

[44] V.S. Zaritskii and L.I. Shimelevich. Monte Carlo technique in problems of optimal data processing. *Automation and Remote Control*, 12:95 – 103, 1975.